

SUPPLEMENTAL MATERIAL

Inspection of the signaling profiles reveals context-dependent regulation of signals

While many signals had activation profiles that matched well with our expectations based on literature reports, others were more surprising. Here, we detail some of these observations.

TNF-induced a biphasic response in IKK activity

In TNF-treated cells, IKK activity showed a biphasic response: IKK was transiently activated early in the time course ($t = 0\text{--}60$ min) followed by a more significant activation at $t > 4$ hr (Figure 4A). We will show elsewhere that IKK activation during the first 60 min of the time course is a direct result of TNF stimulation whereas the late phase activation is mediated by a multistep autocrine cascade involving TGF- α and IL-1 α (1).

ptEGFR is an aggregate measure of phosphorylation and receptor uptake

Unexpectedly, we observed only a small initial increase in ptEGFR in treatments with saturating EGF (Figure S1). On further analysis it became evident that this arises because cells were not starved of serum prior to cytokine addition, as is commonly done in studies of EGF signaling. When cells are not starved, basal EGFR phosphorylation is high as a consequence of autocrine signaling by EGF family members and further increases in phosphorylation are more difficult to detect. The gradual rise in ptEGFR ratios which we observe under sustained EGF stimulation reflects the presence of a constant amount of phosphorylated receptor and a drop in total EGFR levels due to receptor uptake (Figure S1).

→ Figure S1 placement ←

IRS-1 S636 phosphorylation as a negative regulator of the IRS1 Y896 phosphosite

S636 phosphorylation on IRS1 is thought to be mediated by the mTOR pathway downstream of insulin-induced Akt and to negatively regulate IRS1 interaction with the insulin receptor (Figure 1C) (2,3). The phosphorylation of IRS1 on S636 has previously been reported in response to insulin (4) and TNF (5), but not EGF. However, we found S636 phosphorylation to be greatest in response to TNF and EGF and weaker with insulin (Figure S2A and 4A), despite that the presumed activator of mTOR, Akt, was most strongly activated by insulin. These results suggest that TNF and EGF induce mTOR in an Akt-independent fashion in HT-29 cells or, alternatively, that IRS1 S636 phosphorylation is mTOR-independent in these conditions.

The combination of TNF + EGF led to similar levels of phospho-S636 IRS1 as did TNF alone, although this transient pulse of phosphorylation was already initiated by 5 min as it is in treatment with EGF alone (Figure S2A). Interestingly, we observed that TNF cotreatment reduced the levels of the activating IRS1 Y896 phosphorylation induced by EGF (Figure S2B). Serine phosphorylation of IRS1 has been linked to TNF-induced insulin resistance in other cell types (6-10). This raises the possibility that TNF-induced IRS1 S636 phosphorylation may also reduce activation of IRS1 by EGFR (Figure S2C).

→ Figure S2 placement ←

TNF-mediated inhibition of insulin-induced Akt activation in HT-29 cells

TNF-induced insulin resistance had been documented in hepatocytes, myocytes, and adipocytes (6-10). In HT-29 cells, we found that TNF was inhibitory for insulin-mediated Akt activation. Saturating insulin levels induced sustained Akt phosphorylation and activation over a 24-hr period, but in the presence of TNF, Akt activity rose sharply initially but then fell gradually over time until it had returned to basal levels at 24 hr (Figure S3A). Because about

50% of the cells were apoptotic at 24 h in TNF + insulin (as judged by cleaved caspase-3 and cytokeratin levels), one simple explanation for the fall in Akt activity relative to insulin-treatment alone is that Akt is absent from dead or dying cells. However, we found that apoptotic, floating cells and non-apoptotic, adherent cells have indistinguishable Akt levels (Figure S3B). Thus, TNF must deactivate Akt, independently of whether cells are apoptotic (Figure S3C). Because insulin-induced Y896 IRS1 phosphorylation was not measurable in our treatment conditions, it remains to be shown whether the drop in Akt activity in TNF + insulin-treated cells could be linked to inhibition of IRS1 activation by TNF-induced IRS1 Ser phosphorylation (2).

→ Figure S3 placement ←

Receptor saturation does not necessarily equate with signal saturation

Crosstalk between proapoptotic and prosurvival cytokines had distinct effects on signaling dynamics. For ERK, the TNF + EGF combination was partially additive: TNF or EGF alone induced eightfold ERK activation at $t = 15$ min and $t = 5$ min respectively, while cotreatment with saturating TNF and EGF activated ERK tenfold at $t = 5$ min (Figure S4A). These results imply that neither EGF nor TNF fully activated the pool of ERK kinase in these cells, even at concentrations that should saturate receptors (Figure S4B). Similarly, phospho-FKHR levels were maximal in cells cotreated with TNF and EGF (Figure S4C-D).

→ Figure S4 placement ←

Although the dynamics of certain signals such as ERK, pFKHR, pIRS1, and Akt were markedly changed by cytokine cotreatments, others were largely unaffected. For example, TNF potently induced JNK1 and MK2 activity, and these signals were unchanged by insulin and EGF (Figure S4E and 4H) except at near-physiological TNF concentrations (Figure S4F-G, I-J). Overall, the data in the compendium indicate that cytokine regulation of protein signals by

multiple cytokines is complex and likely involves intracellular crosstalk between several pathways. Adding another level of complexity, the interplay between TNF, EGF, and insulin signal transduction networks in HT-29 cells also depends on extracellular crosstalk through autocrine signaling (1).

SUPPLEMENTAL REFERENCES

1. Janes, K. A., Gaudet, S., Albeck, J. G., Nielsen, U. B., Lauffenburger, D. A., and Sorger, P. K. (2005) Autocrine crosstalk in the response of human cells to apoptotic and mitogenic stimuli. Submitted
2. Paz, K., Hemi, R., LeRoith, D., Karasik, A., Elhanany, E., Kanety, H., and Zick, Y. (1997) A molecular basis for insulin resistance. Elevated serine/threonine phosphorylation of IRS-1 and IRS-2 inhibits their binding to the juxtamembrane region of the insulin receptor and impairs their ability to undergo insulin-induced tyrosine phosphorylation. *J Biol Chem* **272**, 29911-29918
3. Harrington, L. S., Findlay, G. M., and Lamb, R. F. (2005) Restraining PI3K: mTOR signalling goes back to the membrane. *Trends Biochem Sci* **30**, 35-42
4. Batty, I. H., Fleming, I. N., and Downes, C. P. (2004) Muscarinic-receptor-mediated inhibition of insulin-like growth factor-1 receptor-stimulated phosphoinositide 3-kinase signalling in 1321N1 astrocytoma cells. *Biochem J* **379**, 641-651
5. Ozes, O. N., Akca, H., Mayo, L. D., Gustin, J. A., Maehama, T., Dixon, J. E., and Donner, D. B. (2001) A phosphatidylinositol 3-kinase/Akt/mTOR pathway mediates and PTEN antagonizes tumor necrosis factor inhibition of insulin signaling through insulin receptor substrate-1. *Proc Natl Acad Sci U S A* **98**, 4640-4645

6. Kanety, H., Feinstein, R., Papa, M. Z., Hemi, R., and Karasik, A. (1995) Tumor necrosis factor alpha-induced phosphorylation of insulin receptor substrate-1 (IRS-1). Possible mechanism for suppression of insulin-stimulated tyrosine phosphorylation of IRS-1. *J Biol Chem* **270**, 23780-23784
7. Aguirre, V., Uchida, T., Yenush, L., Davis, R., and White, M. F. (2000) The c-Jun NH(2)-terminal kinase promotes insulin resistance during association with insulin receptor substrate-1 and phosphorylation of Ser(307). *J Biol Chem* **275**, 9047-9054
8. Gao, Z., Zuberi, A., Quon, M. J., Dong, Z., and Ye, J. (2003) Aspirin inhibits serine phosphorylation of insulin receptor substrate 1 in tumor necrosis factor-treated cells through targeting multiple serine kinases. *J Biol Chem* **278**, 24944-24950
9. de Alvaro, C., Teruel, T., Hernandez, R., and Lorenzo, M. (2004) Tumor necrosis factor alpha produces insulin resistance in skeletal muscle by activation of inhibitor kappaB kinase in a p38 MAPK-dependent manner. *J Biol Chem* **279**, 17070-17078
10. Csehi, S. B., Mathieu, S., Seifert, U., Lange, A., Zweyer, M., Wernig, A., and Adam, D. (2005) Tumor necrosis factor (TNF) interferes with insulin signaling through the p55 TNF receptor death domain. *Biochem Biophys Res Commun* **329**, 397-405

SUPPLEMENTAL FIGURE LEGENDS

Figure S1. EGFR and Akt signals measured by antibody microarray. Heat map of time course signal measurements in 12 treatment conditions. Phosphorylated, total, and phospho-to-total amounts of EGFR and Akt were measured by antibody microarray. For each treatment, the normalized average signal intensities are plotted at each time point (0, 5, 15, 30, 60, 90 min and 2, 4, 8, 12, 16, 20, 24 hr; 0: green; 0.5: black; 1: red).

Figure S2. Regulation of IRS-1 Y896 and S636 phosphosites in TNF- and EGF-treated cells. (A-B) Time courses of IRS-1 phosphorylation at Y896 (A) and S636 (B) in cells treated with 100 ng/ml EGF (red), 100 ng/ml TNF (blue) or 100 ng/ml EGF + 100 ng/ml TNF (black) treated cells. In both graphs, the means \pm S.E.M. of triplicate samples are plotted. (C) Diagram depicting a hypothesized regulatory scheme for IRS1. Saturating TNF reduced the amount of EGF-induced Y896 phosphorylation on IRS1. This inhibition may be mediated by TNF-induced phosphorylation of IRS1 at S636.

Figure S3. TNF-mediated inhibition of insulin-induced Akt activation. (A) Time course of immunoblot phospho-S473 Akt in cells treated with 500 ng/ml insulin (red), 100 ng/ml TNF (blue) or 100 ng/ml TNF + 500 ng/ml insulin (black). (B) Akt signaling is similarly inhibited by TNF in both viable and apoptotic cells. Bar graph comparing Akt activity in dead (floating, grey) and live (adherent, white) cells treated with 500 ng/ml insulin or 100 ng/ml TNF + 500 ng/ml insulin for 24h. In all graphs, the averages \pm S.E.M. of triplicate samples are plotted. (C) Diagram describing how cotreatment with TNF led to gradual reduction in the sustained

phospho-Akt levels induced by saturating insulin in all cells, even as TNF alone induced a small transient Akt activation.

Figure S4. Receptor saturation does not necessarily equate with signal saturation. Time courses of ERK activity (A) and phospho-S256 FKHR levels (C) in cells treated with 100 ng/ml EGF (red), 100 ng/ml TNF (blue) or 100 ng/ml EGF + 100 ng/ml TNF (black). (B, D) Diagrams depicting how TNF indirectly potentiated ERK (B) and phospho-FKHR (D) signals induced by EGF. (E-F, H-I) EGF and insulin inhibition of TNF-induced JNK1 and MK2 signaling is TNF-dose dependent. Time courses of JNK1 (E-F) and MK2 (H-I) activity in cells treated with TNF alone (red), or with EGF (blue) or insulin (black), at saturating (E, H) or low levels (F, I). (G, J) Diagrams describing how cotreatment with EGF and insulin had a weak, but significant, inhibitory effect on JNK1 (G) and MK2 (J) activity induced by TNF. In all graphs, the means \pm S.E.M. of triplicate samples are plotted.

Table S1. Lot-controlled reagents

Reagent	Source	Catalog #	Use	Concentration
Serum	Hyclone	SH30088.03	Culture	10 %
IFN γ	Roche	1050494	Pre-stimulus	200 U/ml
TNF	Peprotech	300-01A	Stimulus	0.2, 5, 100 ng/ml
EGF	Peprotech	100-15	Stimulus	1, 100 ng/ml
Insulin	Roche	1376497	Stimulus	1, 5, 100 ng/ml
IL-1ra	R&D Systems	280-RA	Perturbation	10 μ g/ml
C225 mAb	H.S. Wiley, PNNL		Perturbation	10 μ g/ml
α -Caspase-8 (1C12)	Cell Signaling Tech.	9746	Immunoblot	1:1000
α -phospho Akt (S473)	Cell Signaling Tech.	9271	Immunoblot	1:1000
α -phospho MEK1/2 (S217/221)	Cell Signaling Tech.	9121	Immunoblot	1:1000
α -phospho FKHR (S256)	Cell Signaling Tech.	9461	Immunoblot	1:500
α -Caspase-3	Santa Cruz Biotech.	SC-7272	Immunoblot	1:250
α -phospho IRS1 (S636)	Cell Signaling Tech.	2388	Immunoblot	1:1000
α -phospho IRS1 (Y896)	Calbiochem	GF1003	Immunoblot	1:1000
α -cleaved caspase-3	BD Pharmingen	559565	Flow cytometry	1:250
α -cleaved cytokeratin	BD Pharmingen	12140349	Flow cytometry	1:250
Annexin V	Molecular Probes	A-13201	Flow cytometry	1:20
α -EGFR 111.6	LabVision	MS-378	Antibody array	0.1 μ g/ml
α -phospho EGFR (Y1068)	Biosource Int.	44-788G	Antibody array	1 μ g/ml
α -EGFR 199.12	LabVision	MS-396	Antibody array	300 μ g/ml
α -Akt	Upstate Biotech.	05-591	Antibody array	500 μ g/ml
α -phospho Akt (S473)	Cell Signaling Tech.	4051	Antibody array	0.8 μ g/ml
α -Akt	Cell Signaling Tech	9272	Antibody array	1:100
α -ERK	Upstate Biotech.	06-182	Kinase assay	10 μ g/ml
α -JNK1	Santa Cruz Biotech.	474 571 1648	Kinase assay	10 μ g/ml
α -Akt	Upstate Biotech.	05-591	Kinase assay	10 μ g/ml
α -IKK α / β (H-470)	Santa Cruz Biotech.	SC-7607	Kinase assay	10 μ g/ml
α -MAPKAP	Upstate Biotech.	07-241	Kinase assay	10 μ g/ml
488-goat α -rabbit IgG	Molecular Probes	A-11008	Immunoblot	1:5000
PE-goat α -mouse IgG	Molecular Probes	P-852	Immunoblot	1:5000
488-donkey α -mouse IgG	Molecular Probes	A-21202	Flow cytometry	1:250
647-donkey α -rabbit IgG	Molecular Probes	A-31573	Flow cytometry	1:250

Figure S1

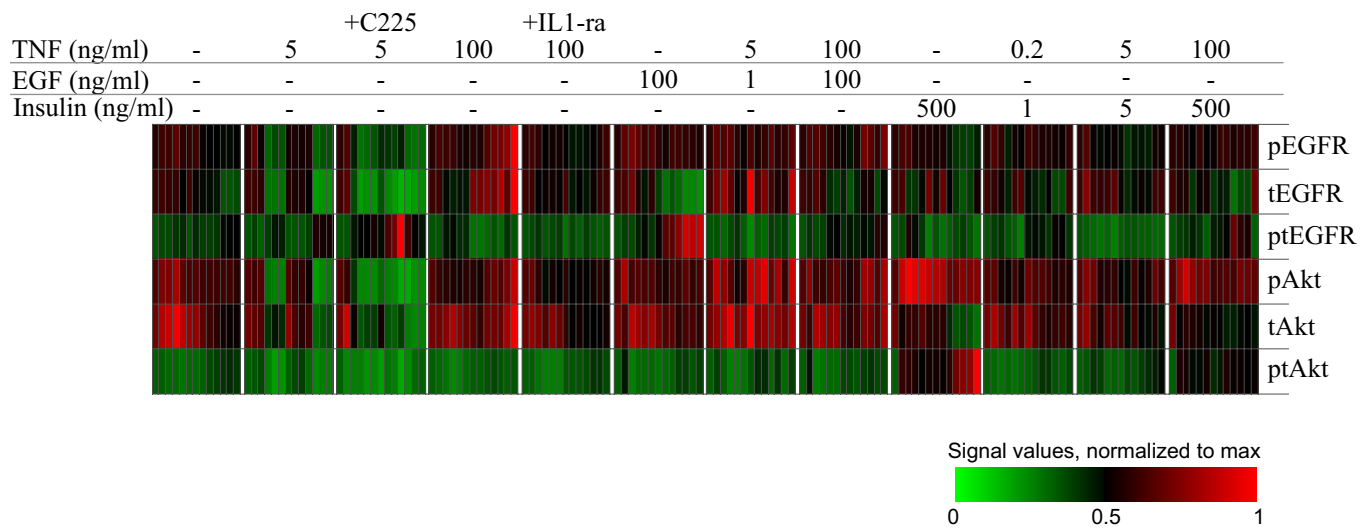


Figure S2

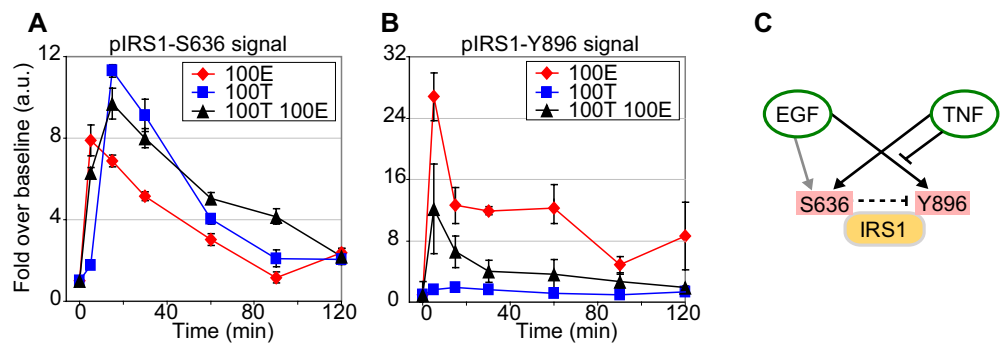


Figure S3

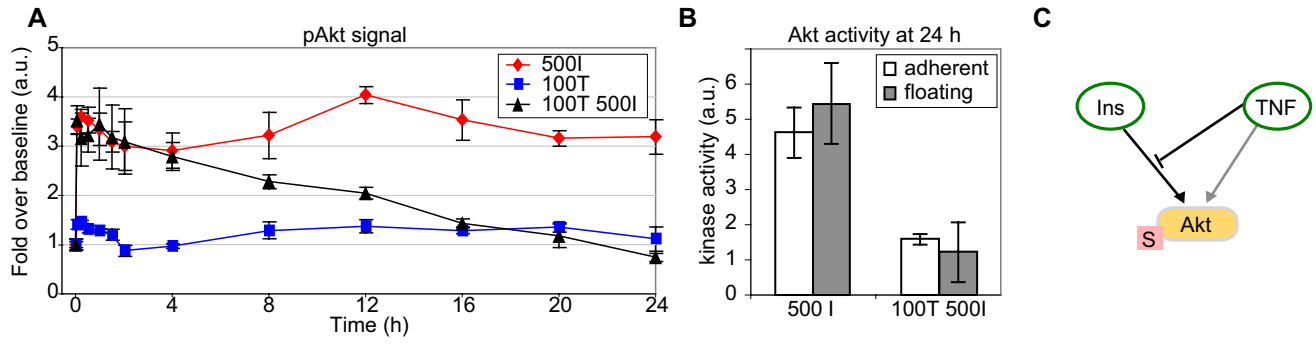


Figure S4

